Quantum spectra of triangular billiards on the sphere

2001 J. Phys. A: Math. Gen. 34 2549

(http://iopscience.iop.org/0305-4470/34/12/303)

INSTITUTE OF PHYSICS PUBLISHING JOURNAL OF PHYSICS A: MATHEMATICAL AND GENERAL

J. Phys. A: Math. Gen. **34** (2001) 2549–2560 www.iop.org/Journals/ja PII: S0305-4470(01)19521-1

Quantum spectra of triangular billiards on the sphere

M E Spina and M Saraceno

Department of Physics, Comisión Nacional de Energía Atómica, Av. Libertador 8250, (1429) Buenos Aires, Argentina

Received 22 November 2000

Abstract

We study the quantal energy spectrum of triangular billiards on a spherical surface. Group theory yields analytical results for tiling billiards while the generic case is treated numerically. We find that the statistical properties of the spectra do not follow the standard random matrix results and their peculiar behaviour can be related to the corresponding classical phase-space structure.

PACS numbers: 0545, 0545P

1. Introduction

The classical dynamics in polygonal billiards (in particular equilateral triangles) on a spherical surface was studied in [1] to investigate the effect of the positive curvature on the classical motion. The structure of phase space for these curved triangular billiards turned out to be regular but very complex. As a consequence of the focusing mechanism on the sphere the phase space is entirely covered by chains of stable islands. Inside each of these islands the motion is elliptic and can be labelled by an infinite repeating code according to the sequence of reflections. This situation which we could call 'piecewise integrable' is very different from that corresponding to plane polygonal billiards, which are either integrable (or pseudointegrable) or ergodic, according to the rationality of their inner angles (see, e.g., [2]). The natural question we would like to answer in this paper is how this peculiar dynamics is reflected in the statistical properties of the quantum mechanical spectrum.

There is much evidence, mainly numerical, that integrable dynamics leads to Poisson statistics while classically chaotic systems satisfy the statistics given by one of the random matrix ensembles (see, e.g., [3]). Mixed systems show a combination of these extremes that depends on the relative size of chaotic and regular regions [4]. On the other hand, a different kind of system, neither regular nor chaotic, has been shown to conform to intermediate statistics: a simple example is the plane pseudointegrable billiard, which has been studied together with other models with similar behaviour by Bogomolny *et al* [5].

The peculiar phase-space structure of equilateral triangles on the sphere led us to believe that their spectral properties would not conform to any universal statistics. In this paper we calculate the quantal energy spectrum and the eigenfunctions of these systems. For generic triangles the calculation will be performed numerically while the spectra of tiling triangles will be derived analytically just by using symmetry arguments, as was the case in the classical counterpart. It was shown in [1] that tiling triangles are very particular systems that not only are integrable but for which only periodic orbits are present. We will see how this peculiarity affects the quantal spectrum. In section 2 we present the model and the numerical procedure to calculate the spectra. Section 3 is devoted to the spectral properties of tiling triangles. In section 4 we derive the level spacing distributions of several generic triangles and discuss them in connection with the corresponding classical phase space. Finally, conclusions are presented in section 5.

2. The model

Given T an equilateral triangle with inner angle ω centred on the north pole of a sphere of radius $R = 1$, we are concerned with the eigenvalue problem

$$\triangle\psi_E + E\psi_E = 0 \quad \text{in} \quad T \qquad \text{and} \qquad \psi_E = 0 \quad \text{on} \quad T \tag{1}$$

where $\triangle$ is the three-dimensional Laplacian in spherical coordinates θ and ϕ given by

$$\triangle = \frac{1}{\sin\theta}\frac{\partial}{\partial\theta}\left(\sin\theta\frac{\partial}{\partial\theta}\right) + \frac{1}{\sin^2\theta}\frac{\partial^2}{\partial\phi^2} \tag{2}$$

and the eigenvalues $E = \frac{2m}{\hbar}\mathcal{E}$, $\mathcal{E}$ being the energies, are dimensionless.

The wavefunction ψ_E can be expanded as

$$\psi_E = \sum_m c_m F^m(E, \cos\theta)\mathrm{e}^{\mathrm{i}m\phi} \tag{3}$$

where m is an integer and F^m is a solution of the Legendre equation

$$\frac{\partial}{\partial x}[(1-x^2)F(x)] + \left[\frac{-m^2}{(1-x^2)} + E\right]F(x) = 0 \tag{4}$$

with $x = \cos\theta$. The functions F^m which have to be regular inside the triangle are then proportional to the Legendre functions of the first kind $P_\nu^m(x)$, with real ν such that $E = \nu(\nu+1)$ and real argument $-1 < x < 1$. These P_ν^m ($m \neq 0$) go to 0 at $x = 1$, while they diverge for $x = -1$.

It will be convenient to define

$$F^m(E, x) = \sqrt{\frac{\Gamma(\nu - m + 1)}{\Gamma(\nu + m + 1)}}P_\nu^m(x). \tag{5}$$

These functions are real for $m \leqslant \nu + 1$ and satisfy the following recursion relation:

$$F^{m+2} = -\sqrt{\frac{1}{(\nu+m+2)(\nu-m-1)}}2(m+1)\frac{x}{\sqrt{1-x^2}}F^{m+1} - \sqrt{\frac{(\nu-m)(\nu+m+1)}{(\nu+m+2)(\nu-m-1)}}F^m \tag{6}$$

which is used in the numerical procedure to compute the F^m.

In order to obtain a spectrum free from the trivial degeneracies due to symmetry we have to desymmetrize the billiard. The spherical equilateral triangle is invariant under the point group C_{3v} and can be cut along the three reflection planes into six triangular subdomains. Solving the eigenvalue problem in each of these irreducible domains with given boundary conditions corresponds to finding a fraction of the spectrum of a given symmetry class. In the following we will treat the Dirichlet problem in the fundamental triangle. This corresponds to solutions which are odd under reflection across all the symmetry planes. Subspectra corresponding to other symmetry classes can be obtained by imposing Neumann and mixed boundary conditions. In the case we are considering the expansion of equation (3) reduces to

$$\psi_E = \sum_p c_{3p} F^{3p}(E, \cos\theta) \sin 3p\phi \tag{7}$$

which vanishes automatically at $\phi = 0$ and $\frac{\pi}{3}$.

In order to solve the problem we use an improved version of the 'point matching' method introduced in [6]. This consists in requiring that the Fourier coefficients of the wavefunction evaluated on the boundary

$$I_n = \int \mathrm{d}s\, \mathrm{e}^{-2\mathrm{i}\pi ns/\mathcal{L}} \psi_E \tag{8}$$

should vanish. $\mathcal{L}$ is the billiard perimeter and ds the line element. The existence of a non-trivial solution leads to the condition

$$\det[J_{n,m}] = 0 \qquad \text{with} \quad n, m = 1, N \tag{9}$$

where

$$J_{n,m}(E) = \int \mathrm{d}s\, \mathrm{e}^{-2\mathrm{i}\pi ns/\mathcal{L}} F^m(E, \cos\theta(s)) \mathrm{e}^{\mathrm{i}m\phi(s)}. \tag{10}$$

Equation (9) determines the energy levels E.

The numerical calculation was performed for equilateral triangles with inner angle $\frac{\pi}{2} \leqslant \omega \leqslant \frac{2\pi}{3}$, that is, fairly large triangles for which no difficulties are expected at the corners. Before presenting these numerical results we analyse in the next section the particular cases of tiling triangles that can be treated analytically.

3. Tiling triangles

As already described in [1] the classical motion in tiling triangles can be studied by following a unique geodesic on the topological surface obtained by sewing together a finite number of replicas of the original billiard. Since the geodesics are closed curves on this compact surface, all orbits are periodic. In other words, every trajectory in a tiling triangle is restricted to a one-dimensional subspace. The system is over-integrable, the compactness of the sphere playing the role of an additional integral. We therefore expect a non-generic behaviour of the level distribution. The eigenvalues and eigenfunctions of tiling triangles can be evaluated by making use of symmetry arguments exclusively. Let us consider the equilateral triangle with $\omega = \frac{\pi}{2}$, that is, a triangle whose vertices coincide with those of a face of an octahedron. Following the desymmetrization scheme of the previous section we cut the triangle into six triangles with Dirichlet boundary conditions and calculate the 'desymmetrized spectrum'. Since the domain tesselates the sphere the solutions of Legendre's equation (4) have to be continuous and one-valued at all points $-1 \leqslant \cos\theta \leqslant 1$. This restricts ν to integer values l and $|m| \leqslant l$. The eigenfunctions sought will then be linear combinations of spherical harmonics Y_l^m that can be determined by requiring that they should vanish on the boundaries. These boundary conditions result in a reduction of the spherical symmetry of the problem: the full spherical symmetry group including all proper and improper rotations in three dimensions will then be reduced to a point group. For this particular triangle it will be the symmetry group of the octahedron. That means that in order to determine the eigenvalue spectrum, that is, the allowed values of l and their degeneracy λ_l, we should determine how each of the representations of the full spherical group $D_l^{\pm}$ may be decomposed into irreducible representations of O_h.

Table 1. First levels of the spectrum of tiling triangles with $\omega = \frac{\pi}{2}$ and $\frac{2\pi}{3}$. The energy of each level is $E = l(l+1)$ and its degeneracy λ_l.

$\omega = \frac{\pi}{2}$		$\omega = \frac{2\pi}{3}$	
l	λ_l	l	λ_l
9, 13, 15, 17, 19	1	6, 9, 10, 12, 13, 14, 15, 16, 17	1
21	2	18	2
23	1	19, 20	1
25, 27, 29, 31	2	21, 22	2
33	3	23	1
35	2	24, 25, 26, 27, 28, 29	2
37, 39, 41, 43	3	30	3
45	4	31, 32	2
47	3	33, 34	3
49, 51, 53, 55	4	35	2
57	5	36, 37, 38, 39, 40, 41	3
59	4	42	4
61, 63, 65, 67, 69, 71	5	43, 44	3
73	6	45, 46	4

The number of times the αth irreducible representation of the subgroup O_h is contained in the representation $D_l^{\pm}$ of the spherical group is given by [7]

$$c_\alpha = \frac{1}{g_{O_h}} \sum_R \chi *_\alpha (R) \chi_l(R) \tag{11}$$

where the sum extends over the elements of the group O_h, the order of which is $g_{O_h} = 24$. The characters $\chi_\alpha(R)$ can be extracted from the corresponding character table while the characters for the proper rotations in the full rotation group are given by [7]

$$\chi[D_l^{\pm}(R_\theta)] = \frac{\sin{(l+\frac{1}{2})\theta}}{\sin\frac{\theta}{2}}. \tag{12}$$

Here R_θ denotes a rotation through θ about some axis. The character of an improper rotation (that is, proper rotation multiplied by an inversion) is the same as the character for the proper rotation for the + representations (that is, for even values of l) and its negative for the $-$ (odd values of l) representation.

By applying the 24 symmetry operations of O_h it can be easily seen that the eigenfunctions satisfying Dirichlet conditions in the reduced triangle transform as the one-dimensional irreducible representation Γ_1^- of O_h. Therefore the degeneracy λ_l of the eigenstate of energy $E_l = l(l+1)$ will be the coefficient of the representation Γ_1^- in the decomposition of $D_l^{\pm}$ according to equation (11).

The first levels of the spectrum are shown in table 1 with their corresponding degeneracies. The eigenfunctions have been obtained by means of diagonalizing the projector of the representation Γ_1^- of O_h: they are the eigenfunctions corresponding to eigenvalues equal to unity. Since the representation is one-dimensional the projector has been expressed in terms of the characters as

$$P_{\Gamma_1^-} = \frac{1}{g_{O_h}} \sum_R \chi_{\Gamma_1^-}(R) D_l^{\pm}(R). \tag{13}$$

Again the sum runs over all the elements of the group, and the D-matrices corresponding to improper rotations are minus those corresponding to proper rotations.

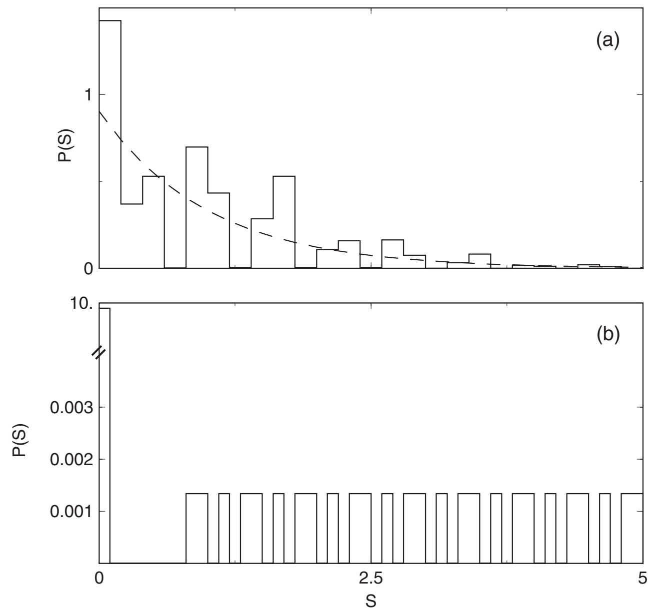

Figure 1. (*a*) The level spacing distribution corresponding to the first 20 000 levels of a desymmetrized plane equilateral triangle. (*b*) The level spacing distribution for the first 7500 levels of a desymmetrized curved tiling triangle with $\omega = \frac{\pi}{2}$.

It is easy to understand that only odd values of l appear in the spectrum of table 1 since the representation Γ_1^- appears only in the decomposition of D representations with negative (natural) parity. Furthermore, it can be seen that for $l \geqslant 13$ all odd values of l are present in the sequence. This means that except for the lowest-lying levels the level spacing $S(l) = E_{l+2} - E_l$ is proportional to l. In order to keep constant the classical mean level spacing $\bar{S}$, which according to Weyl's law is $\bar{S} = \frac{4\pi}{A}$, A being the area of the reduced triangle, the level degeneracy λ_l should also increase linearly with l. The spectrum of the tiling spherical triangle is thus dominated by number-theoretic degeneracies. These 'accidental' degeneracies have been studied by Itzykson and Luck [8]. They appear in some simple integrable quantum systems, for instance, the harmonic oscillator with rational frequency ratios (where $E_{m,n} = m+n+1$) and the plane integrable polygonal billiards (for the equilateral triangle $E_{m,n} = m^2+n^2-mn$). The harmonic potential was extensively investigated by Berry and Tabor [9]. It is an example of overintegrable systems, in which the additional integrals are the conmensurability relations. The spacing among adjacent levels is constant while the degeneracy increases with the energy. This makes the mean level spacing go to zero in the classical limit and no spacing distribution can be defined. The case of the plane equilateral triangle presents more analogy with our case as concerns the mean level spacing $\bar{S}$, which is well defined and given by Weyl's formula. Also there the states are increasingly degenerate and separated by increasingly large gaps.

In order to study the statistics of the nearest-neighbour spacing distribution $P(S)$ we now unfold the spectrum by defining the sequence $e_l = \bar{N}(E_l)$, where $\bar{N}(E)$ is the averaged integrated level density given by

$$\bar{N}(E) = \frac{A}{4\pi}E - \frac{L}{4\pi}\sqrt{E} + \text{const.} \tag{14}$$

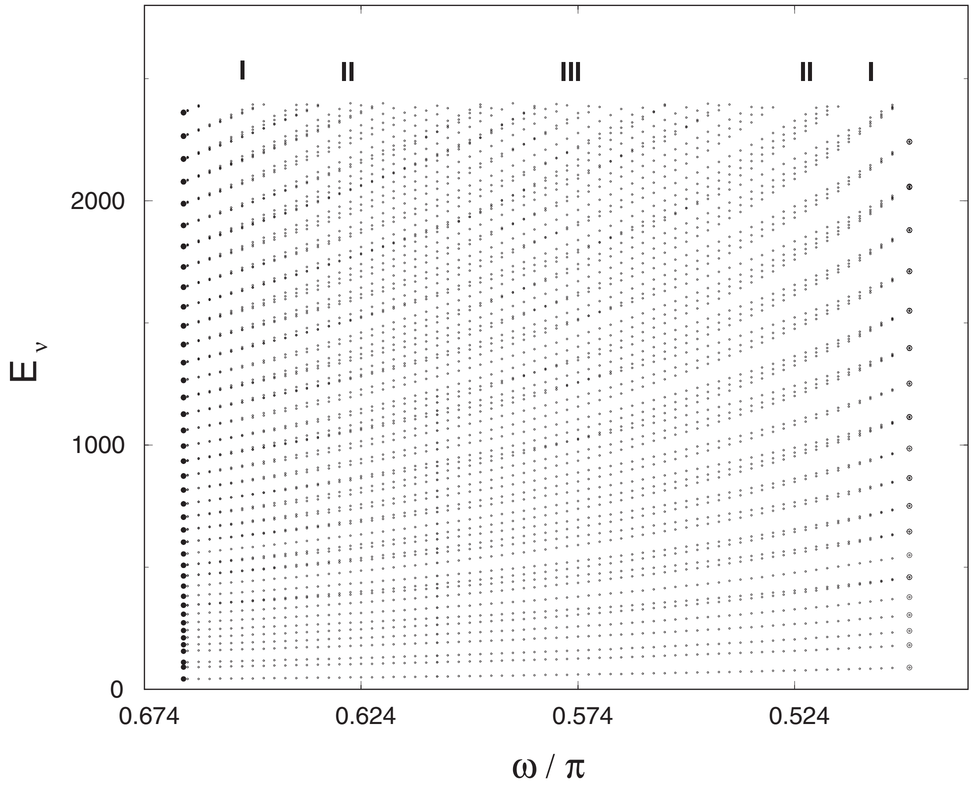

Figure 2. Energy spectra for a family of equilateral triangles with $\frac{\pi}{2} \leqslant \omega \leqslant \frac{2\pi}{3}$. Full points indicate the spectra of the tiling triangles. Region I corresponds to the neighbourhood of tiling triangles, while II and III denote intermediate regions (see text).

L is the triangle perimeter in the spherical metric. The level spacing distribution in the scaled spectrum $P(s)$, with $s_l = e_{l+2} - e_l$, is plotted in figure 1(b) for a sequence of 7500 levels. The distribution is bimodal with a strong tight peak at $s = 0$ and a flat component, giving equal probability to all allowed values of s_l. Since both degeneracies and gaps diverge with the energy this distribution is not defined in the classical limit. Asymptotically the peak tends to a δ-function and the flat mode extends to infinite values of s with a height going to 0. For comparison in figure 1(a) we show the spacing distribution for a sequence of 20 000 energy levels corresponding to a desymmetrized plane equilateral triangle with Dirichlet boundary conditions. Although the distribution looks more Poissonian, as in a generic regular system, the situation is analogous to that in the curved triangle: as shown in [10] degeneracies and gaps diverge with energy. However, as pointed out by Berry in [11] for the similar case of the right plane triangle, this divergence is so slow that this non-generic level structure governed by number-theoretic degeneracies only appears for very high-lying states. Summarizing, the spectrum of tiling spherical triangles is non-generic and, although a mean level spacing can be defined, no spacing distribution $P(s)$ exists in the classical case. This peculiarity is to be attributed to the number-theoretic structure of the spectrum. The spectra of the spherical tiling triangles with angles $\omega = \frac{2\pi}{3}$ and $\frac{2\pi}{5}$ can be calculated in the same way, by considering the symmetry group of the tetrahedron and of the icosahedron respectively. The sequence of eigenvalues corresponding to the desymmetrized triangle with $\omega = \frac{2\pi}{3}$ and Dirichlet boundary conditions, that transform as the one-dimensional irreducible representation Γ_2 of T_d, is presented in table 1. In this spectrum odd and even values of l are allowed. Except for the lowest-lying levels all values of l are present, the level spacing $S(l) = E_{l+1} - E_l$ is again proportional to l and the spectrum has the general characteristics stated above.

4. Generic triangles

The numerical procedure introduced in section 2 was carried out for curved equilateral triangles with inner angle ω ranging from $\frac{\pi}{2}$ to $\frac{2\pi}{3}$. We checked the stability of the solutions by varying the number of points on the boundary used to evaluate the integral in equation (8) and the number of partial waves in the expansion equation (3). The completeness of each spectrum was tested by comparing the calculated cumulative level density $N(E)$ with the averaged one given by the Weyl formula (14). This test is particularly relevant for triangles close to the tiling ones, for which most of the levels are near degenerate and therefore some of them could be missed in the numerical calculation.

In figure 2 we show the energy spectra up to $E = 2400$ for a family of equilateral triangles labelled by ω. These are plotted as curves $E_\nu(\omega)$. The spectra at the left and right boundaries correspond to the integrable triangles with $\omega = \frac{\pi}{2}$ and $\frac{2\pi}{3}$ respectively, which have been evaluated analytically as described in the previous section. The levels in both sequences are labelled by an integer l and their multiplicities increase with energy.

All the remaining triangles with arbitrary rational or irrational angle ω are non-integrable and therefore present no degeneracies in their spectra. Accidental degeneracies are not expected either: by varying ω, we are moving in a one-parameter family and, according to Berry and Wilkinson [12] and references therein, variations in one parameter are insufficient to produce degeneracies. However, in the region denoted as III we observe a great number of quasi-crossings. Their origin will be explained below.

The level spacing distributions corresponding to the unfolded spectra of six triangles with ω ranging from $\frac{\pi}{2}$ to $\frac{2\pi}{3}$ are shown in figure 1. Between 1300 and 2500 levels were considered for each case, except for case (d) ($\omega = 0.589\pi$) where the huge number of quasidegeneracies prevented us to go beyond a few hundreds levels. We observe that the distributions depend drastically on the parameter ω and do not exhibit any universal behaviour. In order to understand the general features of the distributions and their angle dependence we will have to keep in mind the results for tiling triangles derived in the previous section and also refer to the classical phase-space plot which is shown for each case in figure 4. As seen in [1] for generic curved triangles the classical phase space is covered by chains of elliptic islands of regular motion characterized by an infinite repeating code. The multiplicity of these chains increases and their size decreases with the period of the code and phase space takes a fractal structure. As shown in figures 4(a) and (f), for triangles close to the tiling ones phase space is almost dominated by one chain of 3 islands (corresponding to the $+++$ code) in the case $\omega = \frac{\pi}{2}$, and by two chains (corresponding to $+++$ and $+-$) in the case of $\omega = \frac{2\pi}{3}$. The region outside these large domains is entirely covered by 'dust', that is by chains of islands corresponding to very long codes and therefore with extremely high multiplicity and small area. These islands, although regular and of the same type as the dominant ones, cannot be resolved quantum mechanically in the region of the spectrum we are analysing. As we go to triangles far apart from the tiling ones (see figures 4(b)–(e)) other chains of considerable size appear and we will see that some of them can be resolved in the range of energies considered. In order to see how this is reflected in the level spacing distributions we now go back to figure 3.

Histogram (a) corresponds to an angle $\omega = 0.511\pi$ (region I of figure 2) and can be seen as

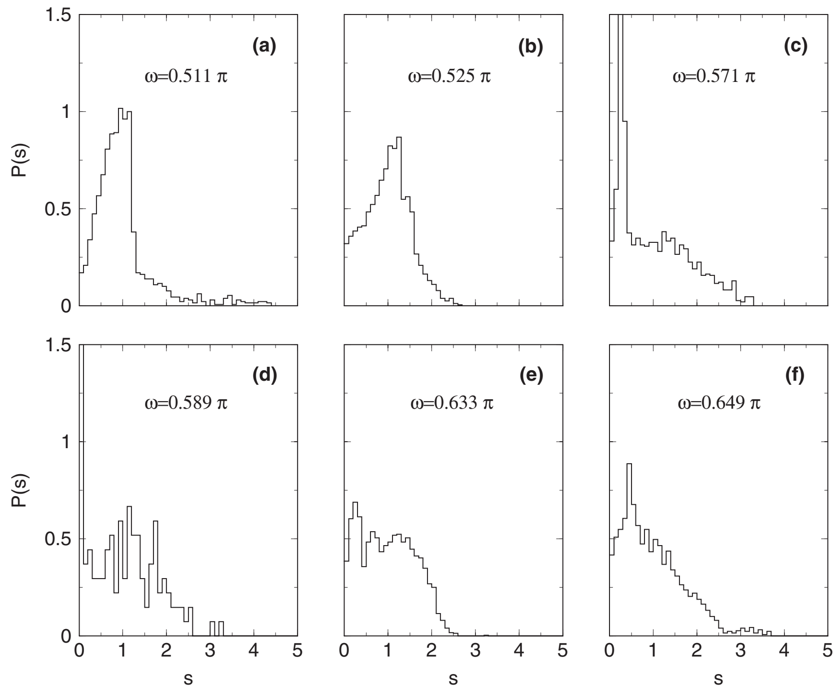

Figure 3. Level spacing distributions for six generic triangles.

a perturbation of the tiling $\omega = \frac{\pi}{2}$. The O_h symmetry is broken and the fact that degeneracies disappear and gaps between levels do not diverge with energy but tend to some finite value reflects in a modification of the distribution of figure 1(a). The distribution figure 3(a) is still bimodal but the delta peak at $s = 0$ is shifted (i.e. there is some level repulsion) and the flat component does not extend to large values of s. Case (f) corresponding to $\omega = 0.649\pi$ (also in region I of figure 2) presents an analogous situation, with a breaking of the T_d symmetry, but in this histogram the low-lying peak is broader (in fact, there is no level repulsion) and the high s-component shows more structure, suggesting a superposition of two uncorrelated spectra. In both cases the distributions, and more specifically the presence or absence of level repulsion, can be better understood by analysing the corresponding eigenfunctions. At a qualitative level, we expect that eigenstates spanning an integrable region will show rigid and regularly spaced spectra. Therefore, in the case where a single integrable region dominates the phase space the spectrum will show repulsion, since all the eigenfunctions are correlated. In contrast, if several classes of eigenfunctions coexist, the distribution can be thought of as a superposition of uncorrelated spectra and there will be no level repulsion. In case (a) the eigenfunctions are of two types: one class lives in the $+++$ elliptic islands, which mostly fill the phase space, the other class extends over the region left outside the islands, which is a very small fraction of the space (see figure 4(a)). Thus, the eigenfunctions of the first class, which are the majority, will be correlated, leading to the level repulsion observed in figure 3(a). In case (f) the eigenfuctions are of three types. Apart from the extended class which lives in the region left outside the islands, there are two classes of localized functions: one living in the $+++$ elliptic islands, the other in the $+-$ islands (see figure 4(f)). Examples of the Husimi representation of functions belonging to these three classes are shown in figure 5. The two classes of localized eigenfunctions living in domains which are comparable in size will be

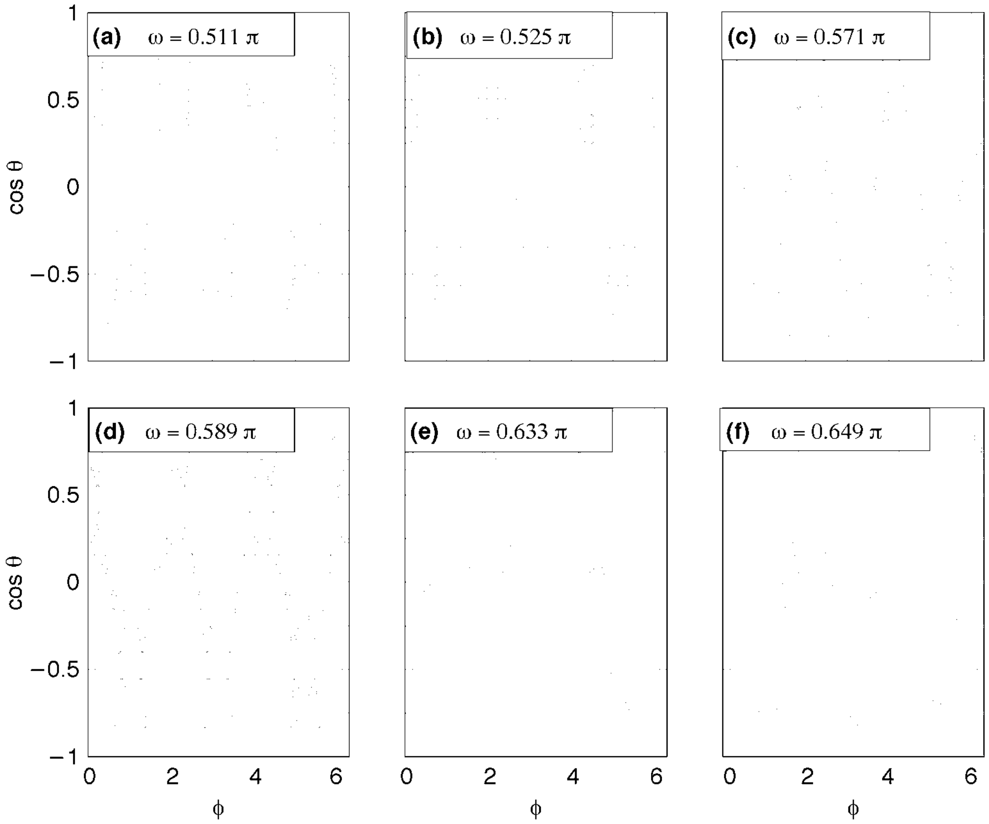

Figure 4. Phase-space plots for six generic triangles.

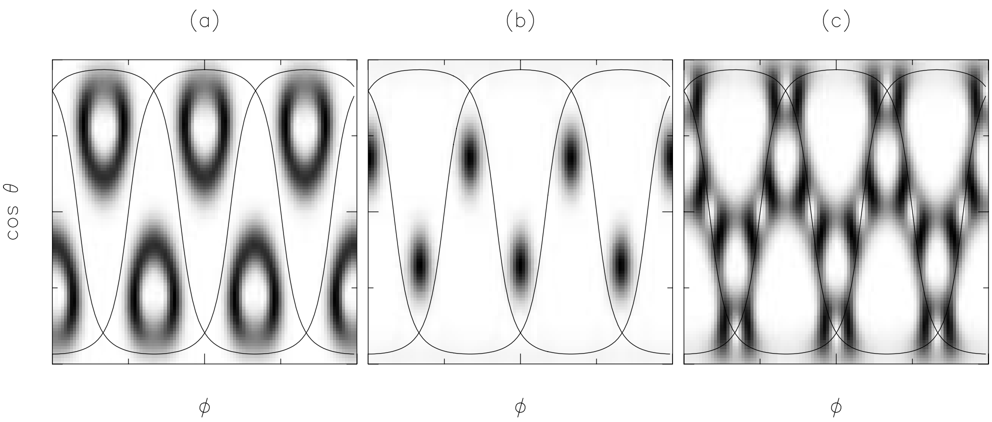

Figure 5. Semiclassical representation of three types of eigenfunction in the triangle with $\omega = 0.649\pi$.

weakly correlated: this explains the much weaker level repulsion in distribution of figure 3(f).

The distributions corresponding to $\omega = 0.525\pi$ and 0.633π are shown in figures 3(b) and (d) respectively. Both correspond to values of the parameter in region II of figure 2. We are now fairly far away from the tiling triangle: the splitting among levels is big, and the two modes have shifted, yielding a single peaked distribution. As we see in the corresponding classical phase-space plot figure 4(*b*) for $\omega = 0.525\pi$ the islands corresponding to codes different from the dominating $+++$ are still small and cannot be resolved in the range of energies we are considering. Still, there are two classes of eigenstates coexisting: those localized in the $+++$ domain, and the extended ones, which now occupy a considerable fraction of phase space. Therefore two classes of weakly correlated eigenfunctions contribute to the spectrum. For $\omega = 0.633\pi$ three classes of functions are present, since the $+-$ islands are large, as shown in figure 4(*d*), and can be resolved.

Summarizing, we can say that the spectra of generic curved triangles are non-universal and follow a parameter-dependent intermediate statistics. The analysis of the corresponding classical phase-space plots suggests that the characteristics of the distributions depend on the number of domains that can be quantum mechanically resolved in a given energy range. The conjecture is the following. If only one large domain is resolved the eigenfunctions in this domain are of the same type and, therefore, correlated. If more than one domain can be resolved, the coupling among states living in different domains will be weak, and the spectrum will be a superposition of uncorrelated spectra, showing no repulsion.

Another interesting observation is the existence of a high peak at a small value of s in the level spacing distributions corresponding to triangles in region III of figure 2. Two examples are shown in figures 3(*c*) and (*d*) for angles $\omega = 0.571\pi$ and 0.589π respectively. This peak is due to the presence of numerous quasi-crossings in this region; the lowest of them are seen already in figure 2. To understand the origin of these quasi-degeneracies we have to refer once again to the classical phase-space plots corresponding to these triangles. As pointed out in [1] generic non-tiling triangles might have domains in which all trajectories are periodic (coexisting with the families of elliptic islands). For example, in all rational triangles with $\omega > \frac{\pi}{2}$ the islands corresponding to the $+-$ code are constituted of periodic orbits. On the other hand, in triangles with inner angle satisfying

$$\cos\frac{\omega}{2} = \sqrt{\frac{3}{4} - \cos^2\frac{k\pi}{n}} \tag{15}$$

all orbits of type $+++$ are periodic with period n.

In region III we find several triangles with rational inner angle or inner angle satisfying equation (15), corresponding to periodic orbits of relatively short period. For example, in case (*d*) ω satisfies equation (15) with period $n = 7$. Although there is no global symmetry group, as in the case of tiling triangles, the presence of these periodic domains, which cover a large fraction of phase space (in particular that corresponding to the $+++$ code), leads to quasi-degeneracies among the quantum states localized in these domains. This is the origin of the huge peak at $s = 0$ in figure 3(*d*). Distribution (*d*) corresponds to an angle close to $\frac{4\pi}{7}$: now the periodic orbits are of type $+-$ with period $n = 7$. Since the area occupied by the $+-$ islands is smaller, the effect is less pronounced: the peak is lower and located at s small but different from zero.

5. Conclusions

In this paper we calculated the quantal spectra of generic and tiling equilateral triangles on a spherical surface. The spectra of the tiling triangles could be obtained analytically by using symmetry arguments while for the generic ones we performed a numerical calculation based on an improved version of the ‘point matching’ method, which allowed us to go up to around 2000 levels.

We found that the spectra of tiling triangles are dominated by arithmetical degeneracies. This is a property shared by other simple quantum systems, in particular by plane square and triangular billiards. In the case of curved triangles the distribution of the degeneracies is easily determined: since the level gap increases linearly with l, that is, it is proportional to $\sqrt{E}$ and the mean level spacing in the classical limit is constant, the degeneracies also increase as $\sqrt{E}$. However, the question asked in [8] about relating these degeneracies to some 'hidden' symmetry also remains open in this case.

As expected, the spectra of generic triangles of variable inner angle ω show no universal behaviour in this energy range. We first remarked that for triangles close to the tiling ones the level spacing distribution is bimodal: this can be seen as a remnant of the level clustering in the tiling systems. More generally, for an interpretation of the spectral properties we had to refer to the corresponding classical phase-space plots. These might be governed by one, or more than one island of considerable size, where considerable means that it can be quantum mechanically resolved in the energy range under consideration. The conclusions seem to be the following. If there is only one resolved domain all the eigenfunctions living in this domain will have support on tori and the corresponding energy levels will be regularly spaced, giving rise to a rigid spectrum. This is the case in triangles with inner angle ω close to $\frac{\pi}{2}$ for which the $+++$ islands covers a great area of the phase space ((a) and (b) in figure 4). If several domains of comparable size coexist different eigenfunctions, which may correspond to levels close in energy, are localized far apart from each other and are weakly correlated. No level repulsion will be present in the spectrum.

In order to check these conjectures and to obtain a quantitative understanding of the spectra we have to extend the calculation to higher energies. The higher we go, the more domains in phase space will be resolved and an increasing number of weakly correlated families of eigenfunctions will be present, localized in these domains. It will then be possible to subdivide the spectrum into subspectra corresponding to each type of eigenfunction (according to their localization in phase space) and study the characteristics of each subspectrum. This subdivision is not possible in this paper since we cannot reach values of k for which the small islands will be explored with significant statistics. To remedy this situation and check whether in the high-k regime the superposition of many uncorrelated spectra recovers asymptotically the Poisson behaviour, we are at present adapting the scaling method [13] to the geometry of the sphere.

Acknowledgments

We are grateful to N N Scoccola for valuable discussions. This work was partially supported by PICT97 03-00050-01015 and CONICET PIP 0420/98.

References

[1] Spina M E and Saraceno M 1999 *J. Phys. A: Math. Gen.* **32** 7803
[2] Gutkin E 1986 *Physica* D **2** 495
[3] Bohigas O 1991 *Proc. 1989 Les Houches Summer School on 'Chaos and Quantum Physics'* ed M J Giannoni *et al* (Amsterdam: North-Holland) p 331
[4] Berry M V and Robnik M 1984 *J. Phys. A: Math. Gen.* **17** 2413
[5] Bogomolny E B, Gerland U and Schmit C 1999 *Phys. Rev.* E **59** R1315
[6] Schmit C 1991 *Proc. 1989 Les Houches Summer School on 'Chaos and Quantum Physics'* ed M J Giannoni *et al* (Amsterdam: North-Holland) p 331
[7] Koster J F, Dimmock J O, Wheeler R G and Statz H 1963 *Properties of the Thirty-two Point Groups* (Cambridge, MA: MIT Press)

[8] Itzykson C and Luck J M. 1986 *J. Phys. A: Math. Gen.* **19** 211
[9] Berry M V and Tabor M 1977 *Proc. R. Soc.* A **356** 375
[10] Pinsky M 1980 *SIAM J. Math. Anal.* **11** 819
[11] Berry M V 1981 *Ann. Phys., NY* **131** 1633
[12] Berry M V and Wilkinson M 1984 *Proc. R. Soc.* A **392** 15
[13] Vergini E and Saraceno M 1995 *Phys. Rev.* E **52** 2204